

# LINC00887 regulates the proliferation of nasopharyngeal carcinoma *via* targeting miRNA-203b-3p to upregulate NUP205

W.-J. YUE<sup>1</sup>, Y. WANG<sup>2,3</sup>, W.-Y. LI<sup>2,3</sup>, Z.-D. WANG<sup>1</sup>

<sup>1</sup>Department of Otorhinolaryngology, The Second Affiliated Hospital, Mudanjiang College of Medicine, Mudanjiang, China

<sup>2</sup>Institute of Neural Tissue Engineering, Mudanjiang College of Medicine, Mudanjiang, China

<sup>3</sup>Department of Anatomy, Mudanjiang College of Medicine, Mudanjiang, China

**Abstract. – OBJECTIVE:** The purpose of this study was to uncover the regulatory effect of LINC00887 on the progression of nasopharyngeal carcinoma (NPC) and the underlying mechanism.

**PATIENTS AND METHODS:** Relative level of LINC00887 in NPC tissues and cells was detected by quantitative real-time polymerase chain reaction (qRT-PCR). Thereafter, the regulatory effect of LINC00887 on proliferative ability in SUNE-1 and HK-1 cells was examined by cell counting kit-8 (CCK-8) and 5-Ethynyl-2'-deoxyuridine (EdU) assay. Through Dual-Luciferase reporter gene assay and RNA-Binding Protein Immunoprecipitation (RIP) assay, the interaction in the regulatory loop LINC00887/miRNA-203b-3p/NUP205 was ascertained. At last, rescue experiments were conducted to clarify the involvement of the regulatory loop LINC00887/miRNA-203b-3p/NUP205 in the progression of NPC.

**RESULTS:** Results showed that LINC00887 was upregulated in NPC tissues and cells, and its overexpression markedly stimulated the proliferative ability in NPC cells. In addition, a potential interaction in the regulatory loop LINC00887/miRNA-203b-3p/NUP205 was discovered, which was responsible for promoting the proliferative ability in NPC.

**CONCLUSIONS:** LINC00887 promotes the proliferative ability in NPC *via* absorbing miRNA-203b-3p to upregulate NUP205.

*Key Words:*

Nasopharyngeal carcinoma, LINC0088, miRNA-203b-3p, NUP205, Proliferation.

## Introduction

Nasopharyngeal carcinoma (NPC) originates from the nasal and pharyngeal epithelial cells, and it is highly prevalent in Asian and North

Africa<sup>1</sup>. Viruses, environmental and genetic factors are all potential pathogenic factors of NPC<sup>2</sup>. Tumor staging and location are two determinants for NPC treatment, and local NPC can be surgically resected. However, under the most circumstances, chemotherapy and radiotherapy are preferred for NPC patients<sup>3,4</sup>.

Long non-coding RNAs (lncRNAs) are non-coding RNAs with over 200 nucleotides long. Increasing evidence has demonstrated the critical significance of lncRNAs in the occurrence and progression of tumor diseases<sup>5,6</sup>. Dysfunctional lncRNAs have been identified in many types of tumor tissues<sup>7,8</sup>. Serum or plasma lncRNAs are highly stable, which are promising indicators and serve as novel tumor biomarkers<sup>9</sup>. Detection of lncRNA-LET, PVT1, PANDAR, PTENP1 and linc00963 could distinguish patients with clear cell renal cell carcinoma from healthy people. Serum level of lncRNA HULC contributes to diagnose and predict the prognosis of gastric cancer<sup>10,11</sup>.

As a tumor-related lncRNA, LINC00887 is able to block the invasion and metastasis of non-small cell lung cancer by degrading corresponding miRNAs<sup>12</sup>. In this paper, LINC00887 was considered to serve as a ceRNA, which promoted the progression of NPC by absorbing miRNA-203b-3p to upregulate NUP205.

## Patients and Methods

### *Sample Collection and Ethical Statement*

NPC tissues and adjacent normal ones were surgically resected from 36 NPC patients. Tissues were frozen in liquid nitrogen and stored at -80°C. Patients and their families have been fully

informed. This investigation was approved by Ethics Committee of The Second Affiliated Hospital, Mudanjiang College of Medicine.

### **Quantitative Real Time-Polymerase Chain Reaction (qRT-PCR)**

TRIzol (Invitrogen, Carlsbad, CA, USA) was applied for isolating cellular RNA, which was quantified using a spectrometer. Then, RNA was reversely transcribed into complementary deoxyribose nucleic acid (cDNA) using the PrimeScript RT reagent Kit (TaKaRa, Otsu, Shiga, Japan). SYBR Premix Ex Taq<sup>TM</sup> (TaKaRa, Otsu, Shiga, Japan) was utilized for qRT-PCR. Finally, the relative level was calculated using  $2^{-\Delta\Delta C_t}$  method, with glyceraldehyde 3-phosphate dehydrogenase (GAPDH) and U6 as internal references. Primer sequences are listed as follows: LINC00887 (Forward): AGAGGGTAGGGGATGGAAGTGG, LINC00887 (Reverse): AGGGATAGCAAA-CACCTAAAATGCA, U6 (Forward): GCTTC-GGCAGCACATATACTAAAAT, U6 (Reverse): CGCTTCACGAATTTGCGTGTCAT, GAPDH (Forward): GAAGAGAGAGACCTCAC-GCTG, GAPDH (Reverse): ACTGTGAGGAG-GGGAGATTCAGT, miRNA-203b-3p (Forward): CAGCGGGTGAAATGTTTAGGAC, miRNA-203b-3p (Reverse): AGTGCAGGGTCCGAG-GT, NUP205 (Forward): GGAAUUAUC-CCAGAACUAAU; NUP205 (Reverse): AGAUG-GUGAAGGAGGAAUAAU.

### **Cell Culture**

NPC cells (HK-1, 5-8F and SUNE-1) and immortalized human nasopharyngeal epithelial cells (NP69) purchased from American Type Culture Collection (ATCC, Manassas, VA, USA) were cultured in Roswell Park Memorial Institute-1640 (RPMI-1640) medium (HyClone, South Logan, UT, USA) containing 10% fetal bovine serum (FBS, HyClone, South Logan, UT, USA), 100  $\mu$ g/mL streptomycin and 100 IU/mL penicillin (Invitrogen, Carlsbad, CA, USA). They were maintained in an incubator with 37°C, 5% CO<sub>2</sub>, and the culture medium was regularly replaced.

### **Cell Transfection**

Cells were inoculated in 6-well plates. On the other day, cells were transfected with 100 nM siRNAs or overexpression vector using Lipofectamine 2000 (Invitrogen, Carlsbad, CA, USA). At 48 h after transfection, the cells were collected for functional experiments.

### **RIP (RNA-Binding Protein Immunoprecipitation) Assay**

RIP assay was performed following the procedures of Millipore Magna RIP Kit (Millipore, Billerica, MA, USA). Cells were incubated with anti-AGO2 or anti-IgG at 4°C overnight. Then, a protein-RNA complex was obtained after capturing intracellular specific proteins by the antibody. Subsequently, proteins were digested by proteinase K and the RNAs were extracted. During the experiment, the magnetic beads were repeatedly washed with RIP washing buffer to remove non-specific adsorption as much as possible. The immunoprecipitant RNAs were finally quantified by qRT-PCR.

### **Cell Counting Kit-8 (CCK-8) Assay**

Cells were inoculated into 96-well plates with  $1.5 \times 10^3$  cells per well. At the appointed time points, 10  $\mu$ L of CCK-8 solution (Dojindo Molecular Technologies, Kumamoto, Japan) was added in each well. Finally, the absorbance at 450 nm of each sample was measured by a microplate reader.

### **5-Ethynyl-2'-Deoxyuridine (EdU) Assay**

Cells were inoculated into a 24-well plate and labeled with 50  $\mu$ M EdU reagent for 2 h. After washing with phosphate-buffered saline (PBS), cells were fixed in 50  $\mu$ L of fixation buffer, decolorized with 2 mg/mL glycine and permeated with 100  $\mu$ L of penetrant. After washing with PBS once, cells were stained with 100  $\mu$ L of 4',6-diamidino-2-phenylindole (DAPI) in dark for 30 min. At last, merged images of EdU-positive (red) and DAPI-labeled cells (blue) were captured under a fluorescent microscope.

### **Dual-Luciferase Reporter Gene Assay**

LINC00887 sequences were amplified and cloned into pMIR-REPORT<sup>TM</sup> vector containing Luciferase vector sequences (5'-...CUCU-CAUUCAUCACUUUUAUCUG...-3'). Mutant LINC00887 was constructed based on the wild-type one using the Phusion Site-Directed Mutagenesis Kit. Then, the cells were co-transfected with wild-type/mutant vector and NC/overexpression vector for 24 h. Subsequently, cells were lysed for measuring relative Luciferase activity (Promega, Madison, WI, USA).

### **Statistical Analysis**

Statistical Product and Service Solutions (SPSS) 22.0 statistical software (IBM, Armonk,

NY, USA) was used for data analysis. All data were expressed as mean  $\pm$  SD (standard deviation). The paired two-tailed *t*-test or chi-square test was used for comparing differences between two groups.  $p < 0.05$  was considered as statistically significant.

## Results

### LINC00887 Was Upregulated In NPC and Promoted Proliferative Ability

Compared with that in adjacent normal tissues, LINC00887 was markedly upregulated in 36 NPC tissues (Figure 1A). Then, it was found that the expression of LINC00887 was not significantly correlated with age, gender, relapse and poor survival, but was related to T stage (tu-

mor extent), N stage (lymph node involvement) and NPC clinical stage (Table I). Consistently, LINC00887 was highly expressed in NPC cells relative to immortalized human nasopharyngeal epithelial cells (Figure 1B). To clarify the biological function of LINC00887, LINC00887 overexpression vector and siRNAs were constructed. Overexpression of LINC00887 vector markedly upregulated LINC00887 in HK-1 cells (Figure 1C). Meanwhile, transfection of three LINC00887 siRNAs all effectively down-regulated LINC00887 level in SUNE-1 cells, and si-LINC00887-3 presented the best efficacy (Figure 1D). It was shown that overexpression of LINC00887 in HK-1 cells increased viability and EdU-positive ratio, while knockdown of LINC00887 in SUNE-1 cells yielded the opposite results (Figure 1E-G).

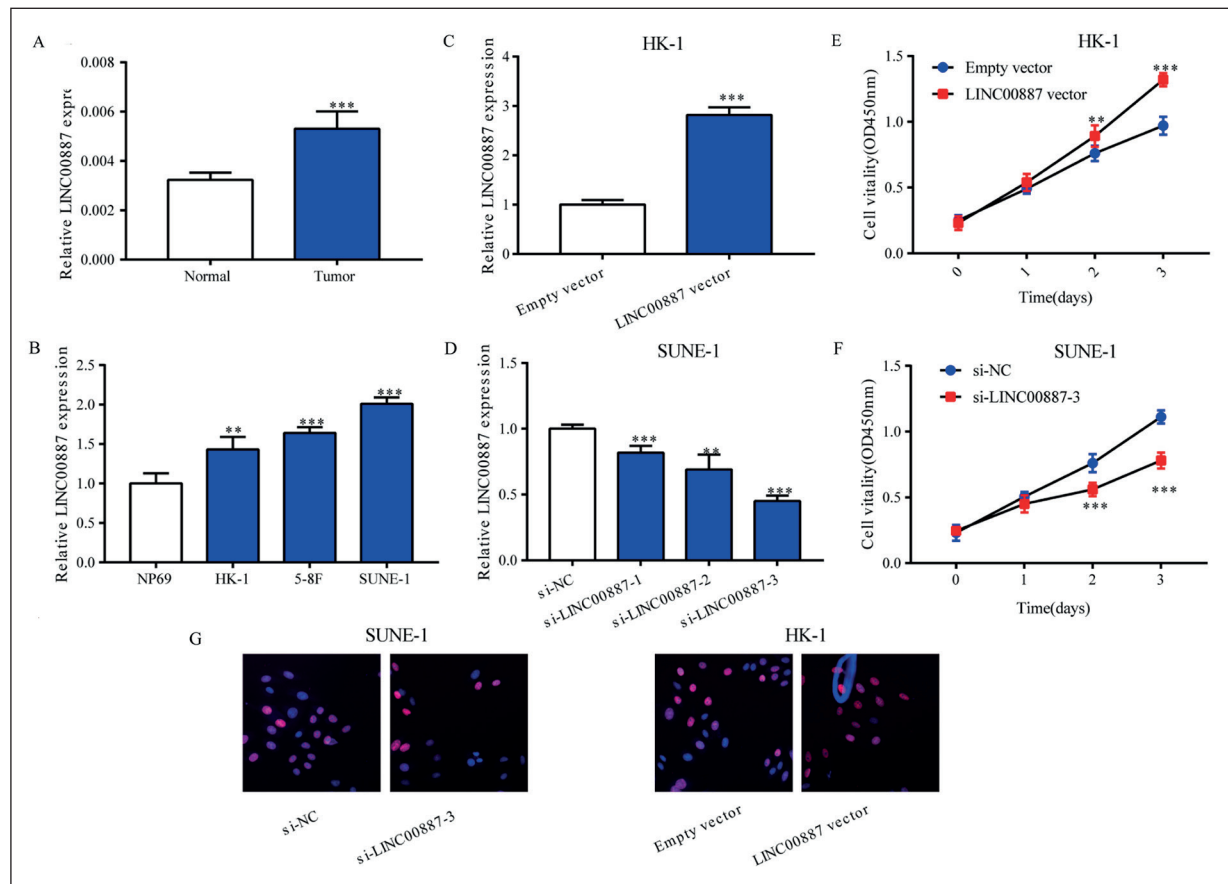


**Figure 1.** LINC00887 is upregulated in NPC and promotes proliferative ability. **A**, LINC00887 levels in NPC tissues and adjacent normal ones. **B**, LINC00887 level in NPC cells and immortalized human nasopharyngeal epithelial cells. **C**, Transfection efficacy of LINC00887 vector in HK-1 cells. **D**, Transfection efficacy of LINC00887 siRNAs in SUNE-1 cells. **E**, Viability in HK-1 cells transfected with empty vector or LINC00887 vector. **F**, Viability in SUNE-1 cells transfected with si-NC or si-LINC00887-3. **G**, EdU-positive ratio in SUNE-1 cells transfected with si-NC or si-LINC00887-3 (left) and HK-1 cells transfected with empty vector or LINC00887 vector (right; magnification: 200 $\times$ ) \* $p < 0.05$ , \*\* $p < 0.01$ , \*\*\* $p < 0.001$ .

**Table 1.** The correlation of LINC00887 expression and clinical characteristics in NPC.

	Cases (n = 36)	LINC00887 expression		p-value
		Low (n = 16)	High (n = 16)	
Age (years)				0.0951
< 50	19	12	7	
≥ 50	17	6	11	
Sex				0.3166
Women	19	11	8	
Men	17	7	10	
T stage (tumor extent)				0.0180*
T1+T2	15	4	11	
T3+T4	21	14	7	
N stage (lymph node involvement)				0.0194*
N0	17	5	12	
N1+N2+N3	19	13	6	
NPC clinical stage				0.0194*
I+II	17	5	12	
III+IV	19	13	6	
Relapse				0.3166
No	19	11	8	
Yes	17	7	10	
Death				0.1715
No	14	5	9	
Yes	22	13	9	

\**p* < 0.05.

### **LINC00887 Served As a miRNA-203b-3p Sponge**

Through online prediction, miRNA-203b-3p was selected as the potential candidate binding LINC00887. Compared with that in adjacent normal tissues, miRNA-203b-3p was downregulated in NPC tissues (Figure 2A). miRNA-203b-3p was downregulated in HK-1 cells overexpressing LINC00887 (Figure 2B). Conversely, miRNA-203b-3p was upregulated in SUNE-1 cells with LINC00887 knockdown (Figure 2C). Based on the binding sites in the promoter regions of LINC00887 and miRNA-203b-3p (Figure 2D), LINC00887-WT and LINC00887-MUT Luciferase vectors were constructed. Decreased Luciferase activity after co-transfection of LINC00887-WT and miRNA-203b-3p mimics verified the binding between LINC00887 and miRNA-203b-3p (Figure 2E, 2F). RIP assay further revealed the interaction between them (Figure 2G, 2H).

### **miRNA-203b-3p Directly Degraded NUP205**

Through TargetScan prediction, NUP205 was selected as the potential downstream gene binding to miRNA-203b-3p. It was found that NUP205

was upregulated in NPC tissues (Figure 3A), and overexpression of LINC00887 markedly upregulated NUP205 level in NPC cells (Figure 3B-3D). Similarly, Dual-Luciferase reporter gene assay verified the binding between miRNA-203b-3p and NUP205 (Figure 3E, 3F). Thus, LINC00887/miRNA-203b-3p/NUP205 regulatory loop was identified.

### **LINC00887/miRNA-203b-3p/NUP205 Regulatory Loop in NPC**

Rescue experiments were conducted to clarify the biological function of LINC00887/miRNA-203b-3p/NUP205 regulatory loop in the progression of NPC. Results revealed that transfection of si-LINC00887-3 markedly downregulated NUP205 level in NPC cells, which was reversed by co-transfection of NUP205 vector (Figure 4A, 4B). Decreased viability in NPC cells with knockdown of LINC00887 was partially reversed by overexpression of NUP205 (Figure 4C, 4D). Similarly, knockdown of LINC00887 reduced EdU-positive ratio, which was further abolished by NUP205 overexpression (Figure 4E, 4F). Hence, it is demonstrated that LINC00887 promotes proliferative ability in NPC by absorbing miRNA-203b-3p to upregulate NUP205.

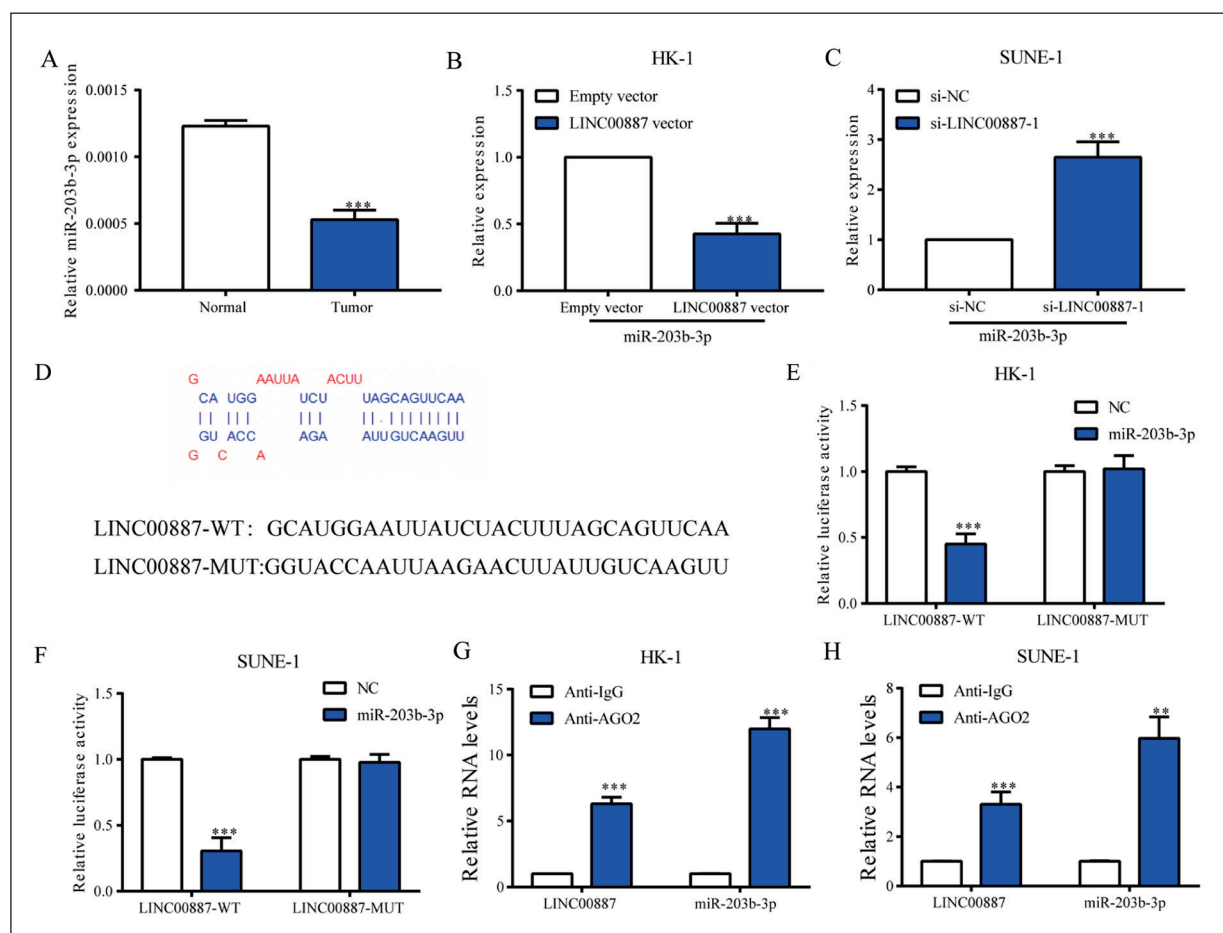


**Figure 2.** LINC00887 serves as a miRNA-203b-3p sponge. **A**, MiRNA-203b-3p levels in NPC tissues and adjacent normal ones. **B**, MiRNA-203b-3p level in HK-1 cells transfected with empty vector or LINC00887 vector. **C**, MiRNA-203b-3p level in SUNE-1 cells transfected with si-NC or si-LINC00887-1. **D**, Potential binding sequences in the promoter regions of miRNA-203b-3p and LINC00887. **E**, **F**, Luciferase activity in HK-1 (**E**) and SUNE-1 cells (**F**) co-transfected with LINC00887-WT/LINC00887-MUT and NC/miRNA-203b-3p mimics. **G**, **H**, Enrichment of LINC00887 and miRNA-203b-3p in anti-IgG and anti-AGO2 in HK-1 (**G**) and SUNE-1 cells (**H**). \* $p < 0.05$ , \*\* $p < 0.01$ , \*\*\* $p < 0.001$ .

## Discussion

The latest evidence has demonstrated the involvement of many lncRNAs in the tumorigenesis of NPC. Serving as oncogenes or tumor-suppressor genes, these lncRNAs provide potential therapeutic and prognostic values. Of note, lncRNA MALAT1 is upregulated in NPC, which affects stem cell phenotypes and radiotherapy resistance *via* targeting the miR-1/slug axis<sup>13</sup>. Knockdown of HOTAIR suppresses invasive ability in NPC by blocking the activation of fatty acid synthases<sup>14</sup>. Overexpression of LINC01420 is closely linked to poor prognosis of NPC<sup>15</sup>. It is reported that LET is downregulated in NPC tissues. Overexpression of LET inhibits proliferative ability and induces apoptosis in NPC cells<sup>16</sup>. As a tumor-suppressor

gene, lncRNA MEG3 suppresses NPC cells to proliferate<sup>17</sup>. The findings of this study demonstrated that LINC00887 was upregulated in NPC, which markedly promoted proliferative ability in NPC cells.

Recently, the ceRNA hypothesis proposes that lncRNAs can regulate target gene expressions by absorbing miRNAs, thus exerting critical functions during tumorigenesis<sup>18</sup>. Based on prediction in Lncbase v.2, potential miRNAs binding LINC00887 were searched and miRNA-203b-3p was selected as a promising candidate. Functional experiments showed that LINC00887 directly bound to miRNA-203b-3p and negatively regulated its level. Notably, LINC00887 promoted proliferative ability in NPC *via* absorbing miRNA-203b-3p as a ceRNA. Nups

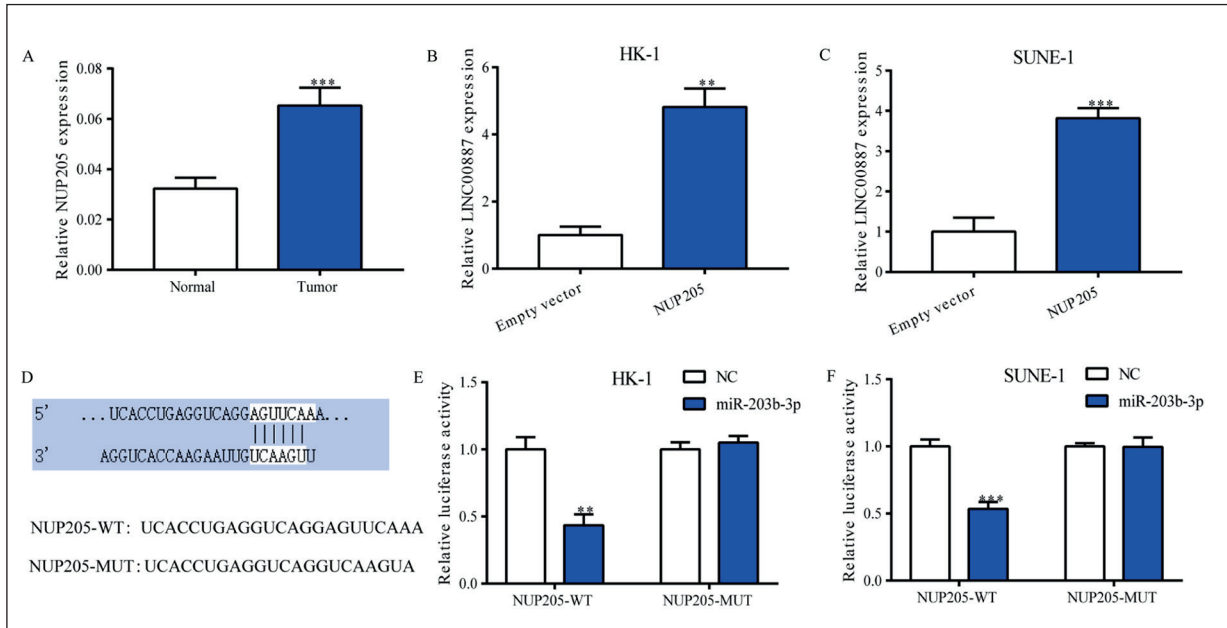


**Figure 3.** MiRNA-203b-3p directly degrades NUP205. **A**, NUP205 levels in NPC tissues and adjacent normal ones. **B**, **C**, NUP205 level in HK-1 (**B**) and SUNE-1 cells (**C**) transfected with empty vector or LINC00887 vector. **D**, Potential binding sequences in the promoter regions of miRNA-203b-3p and NUP205. **E**, **F**, Luciferase activity in HK-1 (**E**) and SUNE-1 cells (**F**) co-transfected with NUP205-WT/NUP205-MUT and NC/miRNA-203b-3p mimics. \* $p < 0.05$ , \*\* $p < 0.01$ , \*\*\* $p < 0.001$ .

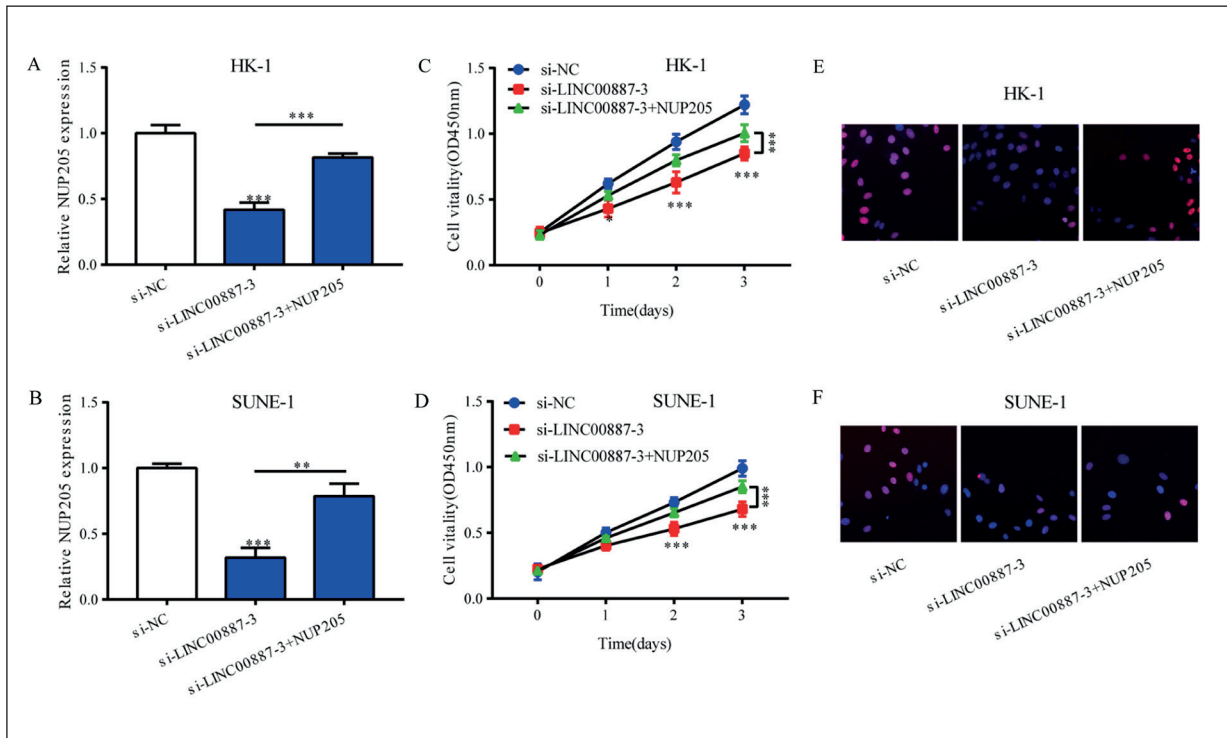


**Figure 4.** LINC00887/miRNA-203b-3p/NUP205 regulatory loop in NPC. HK-1 and SUNE-1 cells were transfected with si-NC, si-LINC00887-3 or si-LINC00887-3 + NUP205 vector. **A**, **B**, Relative level of NUP205. **C**, **D**, Cell viability. **E**, **F**, EdU-positive ratio (magnification: 200 $\times$ ) \* $p < 0.05$ , \*\* $p < 0.01$ , \*\*\* $p < 0.001$ .

(nucleoporins) is defined as a component of the external structure skeleton of the nuclear pore complex or a central pore that mediates the inlet and outlet of the nuclear membrane. NUP205 is one of the components of the central pore that is responsible for the gating function of NPC. Notably, it is not required for the formation or integrity of the nuclear pore complex<sup>19</sup>. Moreover, knockout of NUP205 in *Caenorhabditis elegans* increases the size limit of non-nuclear macromolecules passively entering the nucleus, without influencing active transport of proteins into the nucleus<sup>20</sup>. Therefore, NUP205 alters the dynamics of host cell proteins across the nuclear membrane. In addition, NUP205 is considered as an oncogene to be upregulated in tumor cells. The analysis in this study verified the carcinogenic role of NUP205 in NPC. As the target gene of miRNA-203b-3p, NUP205 was involved in LINC00887-regulated malignant progression of NPC.

### Conclusions

Summarily, LINC00887 promotes the proliferative ability in NPC *via* targeting miRNA-203b-3p to upregulate NUP205. LINC00887 may be utilized as a new hallmark for clinical treatment of NPC.

### Conflict of Interest

The Authors declare that they have no conflict of interests.

### Funding Acknowledgements

This work was supported by the Institute of Neural Tissue Engineering of Mudanjiang College of Medicine, National Natural Science Foundation of China (81870977), the Scientific Research Foundation of Heilongjiang Province, China (LC2017040), the Science Fund of Heilongjiang Provincial Health and Family Planning Commission, China (2018-379).

### References

- KAMRAN SC, RIAZ N, LEE N. Nasopharyngeal carcinoma. *Surg Oncol Clin N Am* 2015; 24: 547-561.
- HE R, HU Z, WANG Q, LUO W, LI J, DUAN L, ZHU YS, LUO DX. The role of long non-coding RNAs in nasopharyngeal carcinoma: As systemic review. *Oncotarget* 2017; 8: 16075-16083.
- CHEN W, HU GH. Biomarkers for enhancing the radiosensitivity of nasopharyngeal carcinoma. *Cancer Biol Med* 2015; 12: 23-32.
- LEE AW, POON YF, FOO W, LAW SC, CHEUNG FK, CHAN DK, TUNG SY, THAW M, HO JH. Retrospective analysis of 5037 patients with nasopharyngeal carcinoma treated during 1976-1985: overall survival and patterns of failure. *Int J Radiat Oncol Biol Phys* 1992; 23: 261-270.
- BO H, GONG Z, ZHANG W, LI X, ZENG Y, LIAO Q, CHEN P, SHI L, LIAN Y, JING Y, TANG K, LI Z, ZHOU Y, ZHOU M, XIANG B, LI X, YANG J, XIONG W, LI G, ZENG Z. Up-regulated long non-coding RNA AFAP1-AS1 expression is associated with progression and poor prognosis of nasopharyngeal carcinoma. *Oncotarget* 2015; 6: 20404-20418.
- GONG Z, YANG Q, ZENG Z, ZHANG W, LI X, ZU X, DENG H, CHEN P, LIAO Q, XIANG B, ZHOU M, LI X, LI Y, XIONG W, LI G. An integrative transcriptomic analysis reveals p53 regulated miRNA, mRNA, and lncRNA networks in nasopharyngeal carcinoma. *Tumour Biol* 2016; 37: 3683-3695.
- YU J, LIU Y, GONG Z, ZHANG S, GUO C, LI X, TANG Y, YANG L, HE Y, WEI F, WANG Y, LIAO Q, ZHANG W, LI X, LI Y, LI G, XIONG W, ZENG Z. Overexpression long non-coding RNA LINC00673 is associated with poor prognosis and promotes invasion and metastasis in tongue squamous cell carcinoma. *Oncotarget* 2017; 8: 16621-16632.
- LI J, WANG X, TANG J, JIANG R, ZHANG W, JI J, SUN B. HULC and Linc00152 act as novel biomarkers in predicting diagnosis of hepatocellular carcinoma. *Cell Physiol Biochem* 2015; 37: 687-696.
- HUANG YK, YU JC. Circulating microRNAs and long non-coding RNAs in gastric cancer diagnosis: An update and review. *World J Gastroenterol* 2015; 21: 9863-9886.
- WU Y, WANG YQ, WENG WW, ZHANG QY, YANG XQ, GAN HL, YANG YS, ZHANG PP, SUN MH, XU MD, WANG CF. A serum-circulating long noncoding RNA signature can discriminate between patients with clear cell renal cell carcinoma and healthy controls. *Oncogenesis* 2016; 5: e192.
- JIN C, SHI W, WANG F, SHEN X, QI J, CONG H, YUAN J, SHI L, ZHU B, LUO X, ZHANG Y, JU S. Long non-coding RNA HULC as a novel serum biomarker for diagnosis and prognosis prediction of gastric cancer. *Oncotarget* 2016; 7: 51763-51772.
- TIAN Y, YU M, SUN L, LIU L, HUO S, SHANG W, SHENG S, WANG J, SUN J, HU Q, DOU Y, ZHU J, REN X, YANG S. Long noncoding RNA00887 reduces the invasion and metastasis of nonsmall cell lung cancer by causing the degradation of miRNAs. *Oncol Rep* 2019; 42: 1173-1182.
- JIN C, YAN B, LU Q, LIN Y, MA L. The role of MALAT1/miR-1/slug axis on radioresistance in nasopharyngeal carcinoma. *Tumour Biol* 2016; 37: 4025-4033.
- MA DD, YUAN LL, LIN LQ. LncRNA HOTAIR contributes to the tumorigenesis of nasopharyngeal carcinoma via up-regulating FASN. *Eur Rev Med Pharmacol Sci* 2017; 21: 5143-5152.

- 15) YANG L, TANG Y, HE Y, WANG Y, LIAN Y, XIONG F, SHI L, ZHANG S, GONG Z, ZHOU Y, LIAO Q, ZHOU M, LI X, XIONG W, LI Y, LI G, ZENG Z, GUO C. High expression of LINC01420 indicates an unfavorable prognosis and modulates cell migration and invasion in nasopharyngeal carcinoma. *J Cancer* 2017; 8: 97-103.
- 16) SUN Q, LIU H, LI L, ZHANG S, LIU K, LIU Y, YANG C. Long noncoding RNA-LET, which is repressed by EZH2, inhibits cell proliferation and induces apoptosis of nasopharyngeal carcinoma cell. *Med Oncol* 2015; 32: 226.
- 17) CHAK WP, LUNG RW, TONG JH, CHAN SY, LUN SW, TSAO SW, LO KW, TO KF. Downregulation of long non-coding RNA MEG3 in nasopharyngeal carcinoma. *Mol Carcinog* 2017; 56: 1041-1054.
- 18) LIZ J, ESTELLER M. lncRNAs and microRNAs with a role in cancer development. *Biochim Biophys Acta* 2016; 1859: 169-176.
- 19) THEERTHAGIRI G, EISENHARDT N, SCHWARZ H, ANTONIN W. The nucleoporin Nup188 controls passage of membrane proteins across the nuclear pore complex. *J Cell Biol* 2010; 189: 1129-1142.
- 20) GALY V, MATTAJ IW, ASKJAER P. Caenorhabditis elegans nucleoporins Nup93 and Nup205 determine the limit of nuclear pore complex size exclusion in vivo. *Mol Biol Cell* 2003; 14: 5104-5115.